

Generation of copper nanoparticles induced by fs-laser irradiation in borosilicate glass

J. M. P. Almeida,¹ L. De Boni,¹ W. Avansi,² C. Ribeiro,³ E. Longo,² A. C. Hernandez¹
and C. R. Mendonca^{1,*}

¹Instituto de Física de São Carlos, Universidade de São Paulo, CP 369, 13560-970 São Carlos, SP, Brasil

²UNESP, Universidade Estadual Paulista, CP 355, 14801-907 Araraquara, SP, Brasil

³EMBRAPA Instrumentação Agropecuária, CP 741, 13560-970, São Carlos, SP, Brasil

*crmendon@ifsc.usp.br

Abstract: Glasses containing metallic nanoparticles are promising materials for technological applications in optics and photonics. Although several methods are available to generate nanoparticles in glass, only femtosecond lasers allow controlling it three-dimensionally. In this direction, the present work investigates the generation of copper nanoparticles on the surface and in the bulk of a borosilicate glass by fs-laser irradiation. We verified the formation of copper nanoparticles, after heat treatment, by UV-Vis absorption, transmission electron microscopy and electron diffraction. A preferential growth of copper nanoparticles was observed in the bottom of the irradiated region, which was attributed to self-focusing in the glass.

©2012 Optical Society of America

OCIS codes: (220.4000) Microstructure fabrication; (190.4720) Optical nonlinearities of condensed matter; (160.2750) Glass and other amorphous materials.

References and links

1. P. P. Prasad, *Nanophotonics* (John Wiley & Sons, Inc, 2004).
2. T. Tokizaki, A. Nakamura, S. Kaneko, K. Uchida, S. Omi, H. Tanji, and Y. Asahara, "Subpicosecond time response of third-order optical nonlinearity of small copper particles in glass," *Appl. Phys. Lett.* **65**(8), 941–943 (1994).
3. C. Silva, J. M. P. Coelho, A. Ruivo, and A. P. de Matos, "Infrared nanosecond laser effects on the formation of copper nanoparticles," *Mater. Lett.* **64**(6), 705–707 (2010).
4. L. De Boni, E. C. Barbano, T. A. de Assumpção, L. Misoguti, L. R. P. Kassab, and S. C. Zilio, "Femtosecond third-order nonlinear spectra of lead-germanium oxide glasses containing silver nanoparticles," *Opt. Express* **20**(6), 6844–6850 (2012).
5. S. L. Qu, Y. C. Gao, X. W. Jiang, H. D. Zeng, Y. L. Song, H. R. Qiu, C. S. Zhu, and K. Hirao, "Nonlinear absorption and optical limiting in gold-precipitated glasses induced by a femtosecond laser," *Opt. Commun.* **224**(4-6), 321–327 (2003).
6. Y. Teng, B. Qian, N. Jiang, Y. Liu, F. Luo, S. Ye, J. Zhou, B. Zhu, H. Zeng, and J. Qiu, "Light and heat driven precipitation of copper nanoparticles inside Cu(2+)-doped borate glasses," *Chem. Phys. Lett.* **485**(1-3), 91–94 (2010).
7. Y. Teng, J. Zhou, F. Luo, G. Lin, and J. Qiu, "Controllable space selective precipitation of copper nanoparticles in borosilicate glasses using ultrafast laser irradiation," *J. Non-Cryst. Solids* **357**(11-13), 2380–2383 (2011).
8. R. R. Gattass, E. Mazur, "Femtosecond laser micromachining in transparent materials," *Nat. Photonics* **2**(4), 219–225 (2008).
9. D. S. Correa, M. R. Cardoso, V. Tribuzi, L. Misoguti, and C. R. Mendonca, "Femtosecond laser in polymeric materials: microfabrication of doped structures and micromachining," *IEEE J. Sel. Top. Quantum Electron.* **18**(1), 176–186 (2012).
10. A. Royon, Y. Petit, G. Papon, M. Richardson, and L. Canioni, "Femtosecond laser induced photochemistry in materials tailored with photosensitive agents [Invited]," *Opt. Mater. Express* **1**(5), 866–882 (2011).
11. D. M. Krol, "Femtosecond laser modification of glass," *J. Non-Cryst. Solids* **354**(2-9), 416–424 (2008).
12. J. R. Qiu, M. Shirai, T. Nakaya, J. H. Si, X. W. Jiang, C. S. Zhu, and K. Hirao, "Space-selective precipitation of metal nanoparticles inside glasses," *Appl. Phys. Lett.* **81**(16), 3040–3042 (2002).
13. J. R. Qiu, X. W. Jiang, C. S. Zhu, M. Shirai, J. Si, N. Jiang, and K. Hirao, "Manipulation of gold nanoparticles inside transparent materials," *Angew. Chem. Int. Ed. Engl.* **43**(17), 2230–2234 (2004).

14. J. Shin, K. Jang, K.-S. Lim, I.-B. Sohn, Y.-C. Noh, and J. Lee, "Formation and control of Au and Ag nanoparticles inside borate glasses using femtosecond laser and heat treatment," *Appl. Phys. A: Mater. Sci. Process* **93**, 923–927 (2008).
15. K. Uchida, S. Kaneko, S. Omi, C. Hata, H. Tanji, Y. Asahara, A. J. Ikushima, T. Tokizaki, and A. Nakamura, "Optical nonlinearities of a high-concentration of small metal particles dispersed in glass: copper and silver particles," *J. Opt. Soc. Am. B* **11**(7), 1236–1243 (1994).
16. J. M. P. Almeida, L. De Boni, A. C. Hernandez, and C. R. Mendonça, "Third-order nonlinear spectra and optical limiting of lead oxifluoroborate glasses," *Opt. Express* **19**(18), 17220–17225 (2011).
17. N. Srinivasa Rao, L. Srinivasa Rao, Y. Gandhi, V. Ravikumar, and N. Veeraiah, "Copper ion as a structural probe in lead bismuth arsenate glasses by means of dielectric and spectroscopic studies," *Physica B* **405**(19), 4092–4100 (2010).
18. A. Lin, B. H. Kim, D. S. Moon, Y. Chung, and W.-T. Han, "Cu²⁺-doped germano-silicate glass fiber with high resonant nonlinearity," *Opt. Express* **15**(7), 3665–3672 (2007).
19. Q. Zhang, G. Chen, G. Dong, G. Zhang, X. Liu, J. Qiu, Q. Zhou, Q. Chen, and D. Chen, "The reduction of Cu²⁺ to Cu⁺ and optical properties of Cu⁺ ions in Cu-doped and Cu/Al-codoped high silica glasses sintered in an air atmosphere," *Chem. Phys. Lett.* **482**(4-6), 228–233 (2009).
20. G. Lakshminarayana and S. Buddhudu, "Spectral analysis of Cu²⁺: B₂O₃–ZnO–PbO glasses," *Spectrochim. Acta, Part A* **62**(1-3), 364–371 (2005).
21. M. Shareefuddin, M. Jamal, and M. Narasimha Chary, "Electron spin resonance and optical absorption spectra of Cu²⁺ ions in xNaI-(30 - x)Na₂O, 70B₂O₃ glasses," *J. Non-Cryst. Solids* **201**(1-2), 95–101 (1996).
22. J. Lakshmana Rao, G. Sivaramaiah, and N. O. Gopal, "EPR and optical absorption spectral studies of Cu²⁺ ions doped in alkali lead tetraborate glasses," *Physica B* **349**(1-4), 206–213 (2004).
23. B. Hua, Y. Shimotsuma, M. Nishi, K. Miura, and K. Hirao, "Micro-modification of metal-doped glasses by a femtosecond laser," *J. Laser Micro/Nanoeng* **2**(1), 36–39 (2007).
24. A. Bishay, "Radiation induced color centers in multicomponent glasses," *J. Non-Cryst. Solids* **3**(1), 54–114 (1970).
25. H. D. Schreiber, M. A. Stone, and A. M. Swink, "Novel red-blue dichroic glass containing copper nanocrystals," *J. Non-Cryst. Solids* **352**(6-7), 534–538 (2006).
26. M. El Sherif, O. A. Bayoumi, and T. Z. N. Sokkar, "Prediction of absorbance from reflectance for an absorbing-scattering fabric," *Color Res. Appl.* **22**(1), 32–39 (1997).
27. F. Gan and L. Xu, *Photonic Glass* (World Scientific, 2006).
28. Y. Dai, G. Yu, M. He, H. Ma, X. Yan, and G. Ma, "High repetition rate femtosecond laser irradiation-induced elements redistribution in Ag-doped glass," *Appl. Phys. B* **103**(3), 663–667 (2011).
29. D. G. Papazoglou and S. Tzortzakakis, "Physical mechanisms of fused silica restructuring and densification after femtosecond laser excitation [Invited]," *Opt. Mater. Express* **1**(4), 625–632 (2011).
30. L. Sudrie, A. Couaillon, M. Franco, B. Lamouroux, B. Prade, S. Tzortzakakis, and A. Mysyrowicz, "Femtosecond laser-induced damage and filamentary propagation in fused silica," *Phys. Rev. Lett.* **89**(18), 186601 (2002).
31. L. Sudrie, M. Franco, B. Prade, and A. Mysyrowicz, "Study of damage in fused silica induced by ultra-short IR laser pulses," *Opt. Commun.* **191**(3-6), 333–339 (2001).
32. A. Mermillod-Blondin, J. Bonse, A. Rosenfeld, I. V. Hertel, Y. P. Meshcheryakov, N. M. Bulgakova, E. Audouard, and R. Stoian, "Dynamics of femtosecond laser induced voidlike structures in fused silica," *Appl. Phys. Lett.* **94**(4), 041911 (2009).

1. Introduction

One of the main interests in metallic nanoparticles arises from the local field enhancement effect that has been used for a number of applications, from sensors to nonlinear optics [1, 2]. The light absorption by nanoparticles produces a coherent and collective oscillation of the electrons, contributing to the enhancement of linear and nonlinear optical properties [1]. These properties are influenced not only by the size and the shape of the nanoparticles, but also by the dielectric environment of the host material [3]. Glasses containing metallic nanoparticles are promising materials for photonic applications because they exhibit ultrafast response times and high third order nonlinearities [4]. There are several ways to obtain metallic nanoparticles in glass; the most common ones are the melt-quenching, sol-gel, chemical vapor deposition and ion exchange [5]. Although these methods provide a considerable management of the quantities and size of the nanoparticles, none of them allow spatial control of the nanoparticles formation, moreover in the micrometer scale [6, 7].

In the last few years, femtosecond laser micromachining has been providing an interesting method to achieve spatial localized modification in materials. In this process, femtosecond pulses are used to induce permanent changes into the bulk or on the surface of materials [8–10]. Due to its nonlinear nature, the material's modification occurs where the

intensity of the light is high enough, i.e., only in the focal volume. Thus, by moving the sample with respect to the laser focus, it is possible obtaining 3D microstructures which can differ from the original material by the refractive index, nonlinear optical susceptibility, crystalline structure, morphology and so on [8, 11]. Nevertheless, the most important process to obtain metallic nanoparticles in confined regions, by femtosecond laser irradiation, is the photo-reduction. The nonlinear interaction between fs-pulses and the glass generates free electrons, which are captured by the metallic cations of the glassy lattice leading to the production of metallic atoms. The aggregation of such metallic atoms is promoted by a thermal process, leading to the metallic nanoparticles precipitation [12, 13].

Recently, several studies on the production of metallic nanoparticles in glass by femtosecond laser excitation have been carried out [12–14]. Most of the papers, however, have been focused on gold and silver nanoparticles, and little attention has been given to copper, which has been shown to present high optical nonlinearities [2]. For example, Tokizaki and co-authors have reported that the third order nonlinear susceptibility of copper nanoparticles is three order of magnitude higher than silver, while it is two orders of magnitude higher than gold [2, 15].

Therefore, this work presents a study on the generation of copper nanoparticles, in a borosilicate glass, induced by fs-laser irradiation and subsequent heat treatment. We have been able to obtain the experimental conditions (laser and heat treatment) to produce spatially localized nanoparticles, in a micrometric scale, on the surface as well as into the volume of the sample. The presence of the nanoparticles was confirmed by absorption and reflectance measurements, and further verified by transmission electron microscopy (average size of 9 nm) and electron diffraction. We also observed a preferential growth of the copper nanoparticles in the bottom of the irradiated region, which we attributed to self-focusing upon the beam propagation in the glass, that present positive nonlinear index of refraction as confirmed by Z-scan measurements.

2. Experimental

A copper doped borosilicate glass ($50\text{SiO}_2 - 17\text{B}_2\text{O}_3 - 11.5\text{MgO} - 10\text{Na}_2\text{O} - 11.5\text{Al}_2\text{O}_3$):0.1CuO mol% was synthesized by conventional melting-quenching technique, using high purity metallic oxides and sodium carbonate as raw material. A batch of 100 g was melted, using a platinum crucible, in an electric furnace open to the atmosphere during 1 h at 1400°C . The resulting melt was quenched into a preheated stainless-steel mold and annealing at 400°C for 12h to minimize the mechanical stress.

Glass transition temperature (T_g) was determined by Differential Scanning Calorimetry (DSC), using a Netzsch STA 409C, in Al_2O_3 pans, within a range of 20 to 700°C with a heating rate of $10^\circ\text{C}/\text{min}$, and in a synthetic air atmosphere. From DSC curve we obtained $T_g = 495 \pm 2^\circ\text{C}$ and no exothermic peak was found, indicating that there is no formation of crystalline phases during the heating up to 700°C .

Polished flat 2 mm thick samples were micromachined using 150 fs, 775 nm laser pulses from a Ti:sapphire amplified system, operating at a 1 kHz repetition rate. The beam was focused beneath and on the sample surface through microscope objectives with numerical apertures (NA) of 0.25 or 0.65. The sample was translated with respect to the laser beam at a constant speed, using a computer-controlled xyz stage. A grating pattern was produced, with approximately 300 lines of 3.2 mm in length, separated by a distance of 15 μm . The pulse energy was measured before the microscope objective and the obtained value was corrected by the corresponding objective's transmittance (63 and 23% for the objectives with NA of 0.25 and 0.65, respectively). Details about the experimental setup used for fs-laser micromachining can be found in ref [9]. After irradiation by fs-laser pulses, the sample was heated for 1 h. The influence of different experimental conditions, such as scanning speed (v), pulse energy (E) and heating temperature, on the Cu nanoparticles generation was investigated.

In order to analyze the surface of the studied samples we performed diffuse reflectance measurement, using a Minolta-CM2600dspectrophotometer equipped with standard D65 (daylight) light source. UV-Vis absorption spectrum measurements were obtained using a Cary 17 spectrometer. Transmission electron microscopy (TEM) images of the copper nanoparticles generated were made using a JEOL JEM 2100 URP equipment. The mean size distribution of the nanoparticles was estimated based on the measurement of at least 100 nanoparticles from TEM images. The nonlinear index of refraction was obtained using closed aperture Z-scan technique. Details about this measurement are described in ref [16].

3. Results and discussion

Figure 1 (curve A) shows the absorption spectrum of the as-prepared copper doped borosilicate glass. The wide absorption band in the range of 550 - 1000 nm is related to Cu^{+2} ions, and confer the bluish color to the sample [3, 17]. Cu^{+2} present unfilled $3d^9$ electron shell and can be coordinated as square planar, tetrahedral and octahedral [18]symmetries. According to some papers, the absorption band around 800 nm is attributed to the electronic transition ${}^2E_g \rightarrow {}^2T_g$ of Cu^{+2} with octahedral symmetry [6, 19]. However, it has been reported that Cu^{+2} is rarely found in regular octahedral site [18, 20]. Previous studies of electron paramagnetic resonance and optical absorption have suggested that the octahedral is tetrahedrally distorted, resulting in a strong elongation along the z-axis [21, 22]. This effect, known as Jahn-Teller, leads to a splitting of 2E_g levels into ${}^2A_{1g}$ and ${}^2B_{1g}$, while ${}^2T_{2g}$ splits into 2E_g and ${}^2B_{2g}$ [17, 20]. Thus, the broad absorption band in the visible and near-IR in Fig. 1 can be attributed to the superposition of ${}^2B_{1g} \rightarrow {}^2A_{1g}$ and ${}^2B_{1g} \rightarrow {}^2B_{2g}$ transitions.

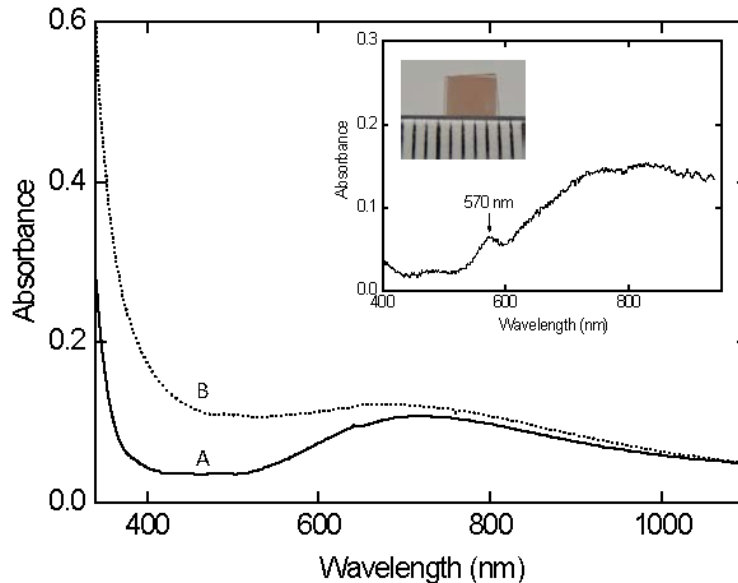


Fig. 1. Linear absorption spectrum of the copper doped borosilicate glass as prepared (curve A), and after the fs-laser irradiation in the bulk using $NA = 0.65$, $v = 100 \mu\text{m/s}$, $E = 90 \mu\text{J}$ (curve B). The inset shows the absorption spectrum and a picture of the irradiated sample after the heat treatment (600°C for 1 h).

After fs-laser irradiation ($E = 90 \mu\text{J}$, $v = 100 \mu\text{m/s}$ and $NA = 0.65$), performed in the volume of the sample at approximately $400 \mu\text{m}$ below the surface, the absorption spectrum exhibits an increase of the absorbance for wavelengths smaller than 700 nm , as observed in Fig. 1 (curve B). Such increase occurs due to color centers formation and photoreduction of Cu^{+2} ions [13, 23, 24]. The photoreduction is a consequence of the free electrons generated

by the nonlinear interaction that results in production of copper atoms (Cu^0). These free copper atoms (Cu^0) have a relatively broad absorption band at around 450 nm, which contributes to the increase in the absorption at the visible region seen in Fig. 1 (curve B) [25]. On the other hand, color centers are lattice defects, such as vacancies, multivalent impurities or non-bridging oxygens which trap electrons and holes generated during the irradiation process, resulting in a preferential light absorption [24]. In general, the identification of the specific defects being induced by fs-laser irradiation for multi-component glasses is a complex task, since many different color centers are generated and, therefore, there is an overlap of their absorption bands. Recent studies, however, have reported mainly the formation of silicon and boron E center, non-bridging oxygen holes center and holes trapped on a single or two non-bridging oxygens [13, 23].

Subsequently to the laser irradiation the samples were subjected to a heat treatment for 1 h at 600° C, in order to promote the aggregation of Cu^0 and, consequently, to the formation of copper nanoparticles. As can be seen by the picture in Fig. 1, after the heat treatment the irradiated region presents a reddish color. The inset in Fig. 1 displays the absorption spectrum of this sample, where a band at 570 nm can be observed. This band is attributed to the surface plasmon resonance (SPR) of copper nanoparticles, responsible for the red color of the glass [6, 7, 23].

The red region of the sample was selected and used to perform TEM and electron diffraction measurements, which are presented in Fig. 2. The TEM image exhibited in Fig. 2(a) confirms the production of copper nanoparticles with an estimated average size of 9 nm, as revealed by the size histogram displayed in Fig. 2(b) (statistics of approximately 100 nanoparticles). The electron diffraction results obtained for the studied sample, depicted in the inset on Fig. 2(a), confirm the formation of a cubic structure for the copper nanoparticles (JCPDS – 04-0836). The diffraction pattern corresponds to a group of precipitates, with almost the same crystallographic orientation. It is not possible affirm that the precipitates are single crystal by the images, however, the good definition of diffraction spots and the small sizes observed indicates that it is very probable. Although this, the presence of a small diffraction halo (as seen for (311) in Fig. 2) indicates that the produced precipitates do not possess a preferential orientation, since they are immobilized in glassy matrix.

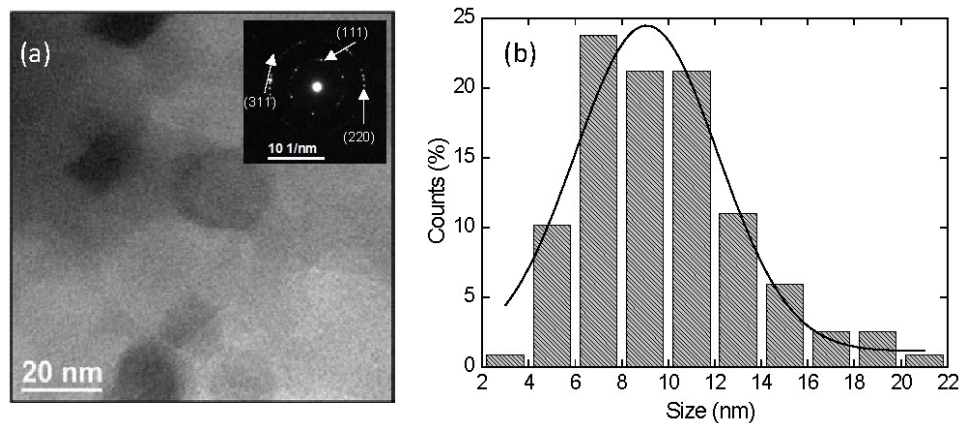


Fig. 2. (a) TEM images obtained from the irradiated sample after the heat treatment. The electron diffraction pattern is shown in the inset; (b) size distribution histogram of the nanoparticles produced.

When fs-laser irradiation is performed on the sample's surface, the irradiated region became opaque due to the surface roughening resulting from material ablation. Therefore, we used diffuse reflectance measurements to verify the appearance of the SPR band. With this measurement it is possible to relate the absorption coefficient (K) to the reflectance (R)

through Kubelka-Munk function $K/S = (1 - R)^2 / 2R$, where S is the scattering coefficient [26]. A comparison between the K/S spectrum of the as-prepared sample (curve A) with the one obtained for the irradiated area after heat treatment at 570°C for 1h (curve B) is shown in Fig. 3. As it can be seen from the inset of Fig. 3, the irradiated area presents a reddish color after the heat treatment as a consequence of copper nanoparticles precipitation, which is confirmed by the SPR band that appear at around 570 nm.

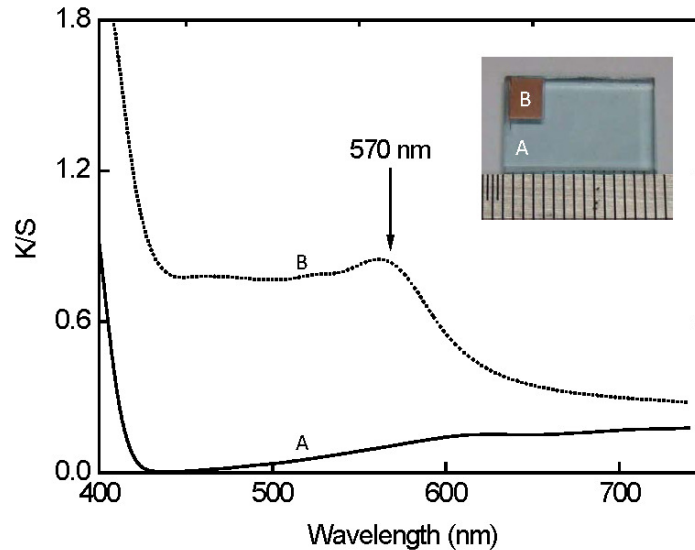


Fig. 3. Kubelka-Munk function (K/S) spectra, obtained from diffuse reflectance measurements, of the as-prepared sample (curve A) and for the sample after irradiation ($E = 260\mu\text{J}$, $v = 1000\mu\text{m/s}$ and $NA = 0.25$) and subsequent heat treatment 570°C/1h (curve B). The inset displays a picture of the sample corresponding to curves A and B.

Concerning the conditions to produce copper nanoparticles, our results indicate that several combinations of the experimental parameters can be used. For $NA = 0.65$, nanoparticles are generated, either in the sample's surface or volume, for pulse energies in the range 20 - 100 μJ , with scanning speeds from 100 until 1000 $\mu\text{m/s}$, although better results were achieved for the slower speeds. When a microscope objective with $NA = 0.25$ was employed, copper nanoparticles were usually observed for energies higher than approximately 200 μJ and scanning speeds faster than 100 $\mu\text{m/s}$. In all cases, the generation of nanoparticles was only observed for a heat treatment with temperatures in the range 570 – 600° C (considering a fixed period of 1 h). Therefore, our results indicate that there is a good range of combinations of the experimental parameters (NA , pulse energy, scan speed and heat treatment temperature) that leads to the formation of the nanoparticles. Moreover, slower scan speed, higher NA and heating temperature favor such formation.

It is important to emphasize that the generation of Cu nanoparticles is only observed in the irradiated areas after the heat treatment. Furthermore, by performing just the heat treatment in the samples (without the laser irradiation) no evidence of nanoparticles formation has been observed. Hence, our results indicate that the generation of copper nanoparticles in borosilicate glasses, induced by low repetition rate fs-pulses, is a two step process. Initially, the high intensity of the fs-laser pulses, achieved at the focal point, generates free electron by photoionization driven by nonlinear interactions [8, 27]. Such free electrons may be trapped, creating color centers, or used in the reduction of Cu^{+2} to Cu^0 (photoreduction reaction $\text{Cu}^{+2} + 2e^- \rightarrow \text{Cu}^0$). After the laser-induced reduction of the copper

ions, the heat treatment enables the atomic mobility required to allow Cu^0 aggregation that results in the formation of copper nanoparticles.

Femtosecond pulses are known to offer high peak power without causing significant damage due to thermal effects, mainly when low repetition rates are used (KHz). Such feature is related to the fact that the light-matter interaction time is shorter than the time in which the energy absorbed by the electrons is transferred to the lattice [8]. When high repetition rate laser (MHz) are employed, however, the cumulative effect from continuous energy deposition results in a heating of the focal zone [28], which can already promote diffusion and aggregation of the metallic atoms and, consequently, nanoparticles growth [6, 7, 28]. Conversely, the thermal effect caused during the irradiation leads to the formation of structures much larger than the spot size of the focused beam [28]. Since our experiments were carried out at a 1 KHz repetition rate, thermal effects caused by light absorption are diminished and, therefore, the photoreduction of the copper ions is confined to the vicinity of the focus, allowing spatial confinement of the copper nanoparticles formation, at micrometer scale, in the bulk or on the surface of the glass.

During the studies on the formation of nanoparticles on the volume of the borosilicate glass, we observed a preferential growth of the copper nanoparticles in the bottom of the microstructured region (3 μm of spacing between lines), as shown in Fig. 4(a). The top view of the glass, after irradiation and heat treatment, exhibits a white color, while the bottom displays a reddish color indicating that the generation of copper nanoparticles occurs preferentially in this region. Figure 4(b) show a lateral view of a glass sample after irradiation (70 μm of spacing between lines) and heat treatment, where again the red color shows up at the lower part of the sample, whereas in the upper portion only a damaged region is observed. Similar results have been recently reported for copper and silver nanoparticles [7, 28], and were attributed to: (i) the non-uniform laser intensity distribution which favors the nanoparticle generation at the lower region and (ii) a higher temperature at bottom part of the structure, achieved with high repetition rate lasers, that favors the growth of nanoparticles in this region. However, since we obtained the same type of profile using a low repetition rate laser, the second hypotheses could be ruled out. Therefore, we believe that cross-section profile observed in Fig. 4(b) is related to filamentation well above the critical power in a transparent solid medium. Because of the self-focusing effect, the intensity rapidly increases (indicated by the damage region in the upper part of Fig. 4(b)) and, consequently, higher order effects, such as multiphoton ionization, leads to plasma generation. Such process arrests the collapse and lead to a propagation region with dynamically regularized intensity [29–32]. Of course, such interpretation only holds if the material presents a positive nonlinear index of refraction ($n_2 > 0$). To verify that, we performed closed aperture Z-scan measurements at 775 nm, using the same laser employed for the micromachining. We observed that the copper doped borosilicate glass presents a positive n_2 , whose magnitude is $3.10^{-20} \text{ m}^2/\text{W}$ (same order of magnitude of fused silica), which supports the proposed mechanism.

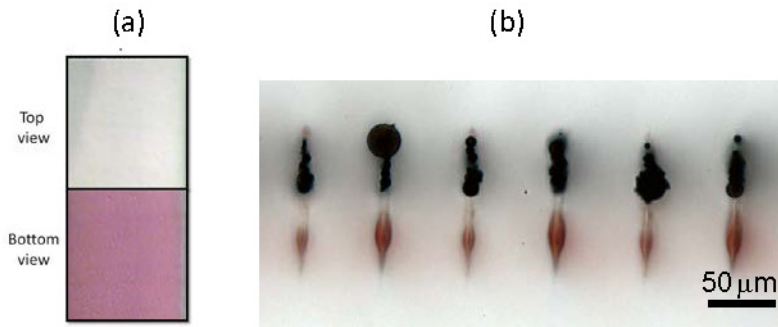


Fig. 4. (a) Top and bottom view images of the sample after irradiation ($E = 100\mu\text{J}$, $v = 100\mu\text{m/s}$, $NA = 0.65$ and $3\mu\text{m}$ of spacing between lines) and heat treatment. (b) Lateral view of the sample after nanoparticles generation ($70\mu\text{m}$ of spacing between lines).

4. Conclusion

The generation of copper nanoparticles in the bulk and on the surface of the copper doped borosilicate glass by femtosecond laser irradiation and subsequent heat treatment was studied. TEM images confirmed the presence of nanoparticles with an average size of 9 nm, while electron diffraction and optical analysis confirmed that the nanoparticles are definitely composed of metallic copper atoms. We also show that several combinations of the experimental parameters leads to the production of the nanoparticles. A preferential growth of nanoparticles in the bottom portion of the microstructured region was observed, which was attributed to a self-focusing effect as the beam propagates through the sample.

Acknowledgments

The authors gratefully acknowledge the financial support from the Brazilian research funding agencies FAPESP, CAPES, CNPq and AFOSR from USA. Authors would also like to thank the Electron Microscopy Laboratory (LME) of the Brazilian National Synchrotron Light Laboratory (LNLS) for the use of the TEM facility.